

Potential-Barrier Effects in Photoabsorption. II. Interpretation of Photoabsorption Resonances in Lanthanide Metals at the $4d$ -Electron Threshold

Jack Sugar

National Bureau of Standards, Washington, D.C. 20234

(Received 28 June 1971)

The resonances in the photoabsorption spectra of the lanthanides near the $4d$ absorption edge are interpreted as transitions of the type $4f^{10}4f^N \rightarrow 4d^9 4f^{N+1}$. Calculations of the $4d^9 4f^{N+1}$ energy levels and relative gf values for these transitions are shown to be in good agreement with the observed absorption spectra. The assumption that the lanthanides occur in trivalent form (with the exception of Eu and Yb) in the metallic solid state is confirmed by these results.

INTRODUCTION

Measurements of absorption peaks in the soft-x-ray range of 100–200 eV have been reported for twelve rare-earth metals.¹ For each metal there appears a group of weak narrow resonances near the $4d$ absorption edge, and for all but Er, Tm, and Yb a broad strong absorption feature appears at higher energy beyond the $4d$ edge. The experiment was later repeated for Ce through Sm and showed the same structure.²

The authors of Ref. 1 suggested that the weak resonances are possibly ionic transitions of the type $4d^{10}4f^N \rightarrow 4d^9 4f^{N+1}$. An analysis of these data led us to the concept of effectively free ions of the triply ionized species in their ground state essentially unperturbed by their metallic environment.³ Calculations of the energy-level structure of the $4d^9 4f^{N+1}$ configuration for four of the cases for which absorption was reported account for nearly all the observed resonances. In fact, the broad peak that was thought to be a feature of the continuum in Refs. 1 and 2 was found to originate from the level structure of $4d^9 4f^{N+1}$. The present paper gives the details of these calculations and applies the method to four more of the absorption spectra reported in Ref. 1.

In this treatment the radial energy integrals are considered as adjustable parameters. They are evaluated by fitting the eigenvalues of the energy matrices to the observed resonances. A comparison of our resulting values for these integrals with those obtained by Hartree-Fock (HF) calculations shows that our fitted values absorb a great deal of configuration interaction. The exchange integral $G^1(fd, df)$ is reduced by ~33% from its value obtained through HF calculations.

The relative oscillator strengths calculated by use of the fitted eigenvectors are in surprisingly good qualitative agreement with the observed data indicating that there is no major distortion of the free-ion structure by the continuum or by local metallic fields. The procedure for a more detailed calculation, including the interaction of the discrete

levels with the continuum, is given in Paper I of this series.⁴

ASSUMPTIONS

Before proceeding with the calculations we must establish the identity of the absorbing levels. This requires the determination of the effective ionization stage of the atom in the metal and a knowledge of the energy levels populated. Zachariasen⁵ has demonstrated a relationship between the metallic radius and the number of s , d , and f electrons present in the metallic state. He found that there is a parallel decrease in the atomic radius as s and d electrons are added to the two long periods beginning with rubidium and cesium, but that when $4f$ electrons begin to appear in the cesium period, the radius decreases much more slowly. He attributed the greater decrease for s and d electrons to the fact that these participate in bond formation while f electrons do not. The break in the cesium sequence occurs at lanthanum at a valency of three, and the radii remain relatively constant thereafter with anomalously large values at Eu and Yb attributed to a return to divalency. This notion suggests that the lanthanides, with the exceptions of Eu and Yb, are effectively triply ionized in the metal. For the present analysis, this will be assumed.

The second assumption is that all observed lines arise from absorption by ions in the ground state. The structure of the ground configurations of the triply ionized lanthanides is now well established.⁶ The position of the first excited level relative to the ground state (omitting Eu) varies from ~1000 cm^{-1} for Sm to ~32 000 cm^{-1} for Gd. If we use the Boltzmann factor for estimating the population of states at room temperature, we find that there is negligible population above the ground state of these ions. We will make this assumption and depend on the fit of observed absorption spectra for confirmation.

COMPUTATIONS

The transitions contemplated are to configurations of the type $4d^9 4f^{N+1}$, where N varies from 0 for La

to 13 for Yb. Applying the Racah tensor operator methods⁷ we evaluate the angular part of the energy matrices and leave the radial integrals as parameters to be adjusted to fit the observed data. The simplification introduced by Fano, Prats, and Goldschmidt⁸ for reducing the recoupling, needed to associate the interacting electrons, to one recoupling coefficient was used. This coefficient was then evaluated by the diagram methods of Jucys *et al.*⁹ The electrostatic coefficient matrices within the f^N core were taken from published data.¹⁰

The fitting procedure requires initial estimated values for the radial integrals. With these, the energy matrices are diagonalized and the resulting eigenvalues are compared with the absorption resonance energies, assuming that each resonance represents an energy level of the upper configuration. This assumption is a simplification since the absorption is continuous and the peaks are actually blends. However, it permits one to determine the underlying discrete structure to a close approximation. After associating the predicted energy levels with the data we then adjust the parametrized radial integrals to values compatible with the observed structure, as has been described by Racah.¹¹ All observed peaks were then used with equal weight in the fitting process. Initial values for the Slater integrals arising from the f - d interaction were calculated by HF methods using the computer code written by Froese.¹² Experience has shown that values obtained from this type of calculation are often too large and we therefore reduced them initially by 25%. This phenomenon may be attributed to the fact that the fitting of Slater integrals tends to absorb effects of configuration interaction

whereas the HF calculation accounts for a pure configuration.

The spin-orbit radial integrals were obtained from observed data. For the $4d^9 2D$ splitting we used the x-ray emission data compiled by Bearden¹³ to obtain end points for an interpolation curve across the lanthanide period. The result is shown in Fig. 1, which was obtained by using the only available pertinent data points from Cs, Ba, and Lu and approximating the usual quadratic shape of such curves. For Cs and Ba we obtained the $4d^9$ splitting from the line interval $N_{IV}O_{III}-N_V O_{III}$. For Lu we had only the lines $N_{IV}N_{VI}$ and $N_V N_{VI, VII}$. If one assumes that $N_V N_{VI}$ was too weak to observe (since it is the off-diagonal transition), the second line was mainly $N_V N_{VII}$. Combining this with the known splitting¹⁴ of $4f^{13} 2F$ in Lu^{4+} we deduced that the $4d^9 2D$ splitting is 9.9 eV. The assumption was made, in utilizing emission data for absorption, that the $4d$ shell is not subject to shielding changes by the $4f$ electrons, since in absorption we have $(N+1)$ $4f$ electrons and in emission we have N $4f$ electrons.

There remain the parameters of the $4f^N$ shell, namely, E^1 , E^2 , E^3 , and ζ_{4f} . The E^k are linear combinations of the Slater parameters F^k defined by Racah.⁷ These have been obtained experimentally for triply ionized lanthanides from crystal spectra⁶ and were utilized here as follows: Since in absorption a hole is left in the atomic core and an additional $4f$ electron is added to the $4f$ shell, the interaction strengths are probably close to those of the next-heavier member of the period. Therefore, we took parameter values for the $4f^N$ lanthanide from the $4f^{N+1}$ lanthanide.

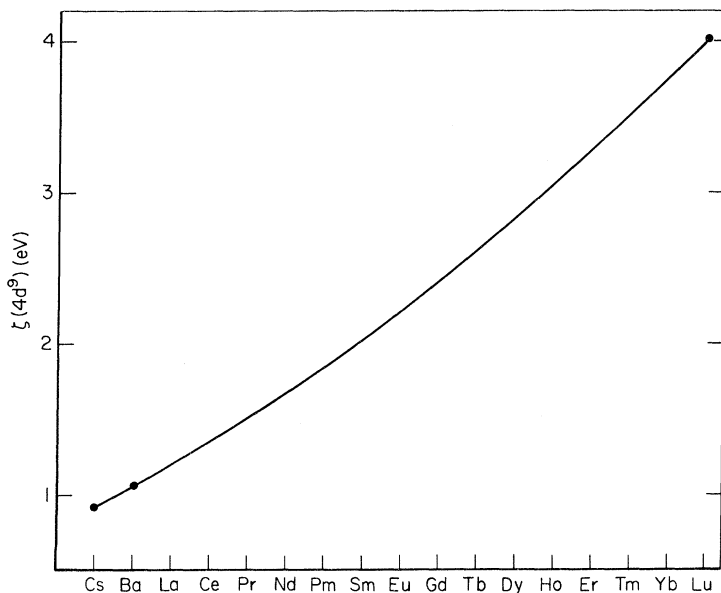


FIG. 1. Interpolation curve for values of the spin-orbit radial integral $\zeta(4d^9)$ for the $4d^9 4f^N$ configurations of the lanthanides.

The fitting procedure was carried a step further, and this proved to be crucial in identifying levels for all spectra more complicated than those of La and Tm. We calculated the dipole line strengths in L - S coupling and transformed them to the actual coupling scheme by means of the eigenvectors which were obtained in the matrix diagonalization. This procedure was described by Cowan¹⁵ in a paper in which he gave some line strength formulas for special cases. One of these, for the case $l_1^m l_2^{m-1} - l_1^{m-1} l_2^m$, was utilized for the present work. We then attempted to identify the observed peaks with the few calculated *strong* lines. These identifications would otherwise be practically impossible to make. In a complicated configuration subject to intermediate coupling one cannot reliably guess in advance which levels will produce strong lines.

Owing to the small number of absorption lines (energy levels) available for fitting, the number of variables in the least-squares adjustment of parameters had to be drastically reduced. The usual procedure is to fix the values of parameters whose contribution to the energy levels is relatively small. As emphasized in Ref. 3, the most important interaction found in these spectra is the exchange represented by G^k , which causes the high-energy absorption peak to appear in most of the lanthanides. The weakest are the interactions within the $4f^N$ core. These $4f^N$ core parameters were fixed in all calculations.

The spin-orbit interaction of the $4d^9$ electrons is also relatively weak and sufficiently well estimated in Fig. 1 to be kept fixed. The ratios among the F^k and G^k parameters were fixed at the ratios given by the HF calculation. Finally, only in the cases of Ce and Pr are the observed levels sufficiently differentiated by F^2 to permit an experimental determination of this interaction. For other cases, its ratio to the HF value obtained by fitting

Ce and Pr was utilized to fix its value.

The HF calculations were made only for La and Tm. For the rest, linearly interpolated values of F^k and G^k were used for the initial parameters. The adjustment of F^2 in Ce and Pr showed that the HF values must be reduced by 25%, as initially guessed. The value of G^1 was deduced in all cases except for Ho and was found to be uniformly overestimated in the HF calculation by about $\frac{1}{3}$. The regularity in the variation of these fitted parameters across the period gave added confidence in the correctness of the level identifications.

RESULTS

The absorption spectra for three sample cases are compared with the calculated positions and relative oscillator strengths in Figs. 2-4. Figures 2 and 3 are Ce and Pr taken from Ref. 2 and Fig. 4 is Er from Ref. 1. The Ce and Pr diagrams are divided at the dashed line where the scale of both the ordinate and the abscissa change to accommodate the wide high-energy peak containing most of the oscillator strength. The vertical lines represent the calculated spectrum with peaks given by the gf (relative) scale. The adjacent scale (where μ is in units of 10^5 cm^{-1}) denotes measurements of absolute absorption coefficients for Ce and Pr. In the case of Er, μ_x is a relative scale. The correspondence between calculated relative gf values and the data for the other spectra is equally as good as those shown.

The values for the radial integrals used in the final diagonalizations of $4d^9 4f^{N+1}$ are given in Table I for the cases studied: La, Ce, Pr, Eu, Gd, Ho, Er, and Tm. The parameter G^1 was adjusted to fit the data in all cases. The standard error in G^1 given in Table I results from the least-squares fitting of this parameter. For Ce and Pr the dependency of the data on F^2 was sufficiently varied so as to permit its value to be determined. The

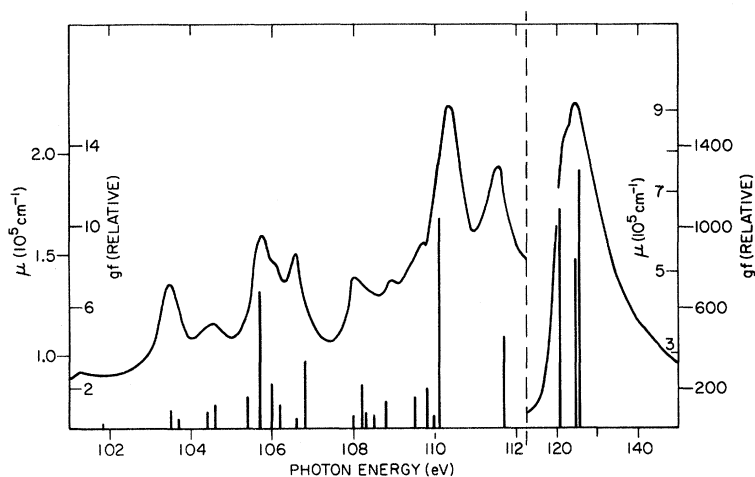


FIG. 2. Comparison of μ , the measured photon absorption coefficient for Ce in the region of the $N_{IV,V}$ edge from Ref. 2, with the calculated relative positions and gf values of the $4d^{10}4f^2 F_{5/2} \rightarrow 4d^9 4f^2$ transitions. A change of scale at the onset of the broad absorption peak is denoted by the dashed line.

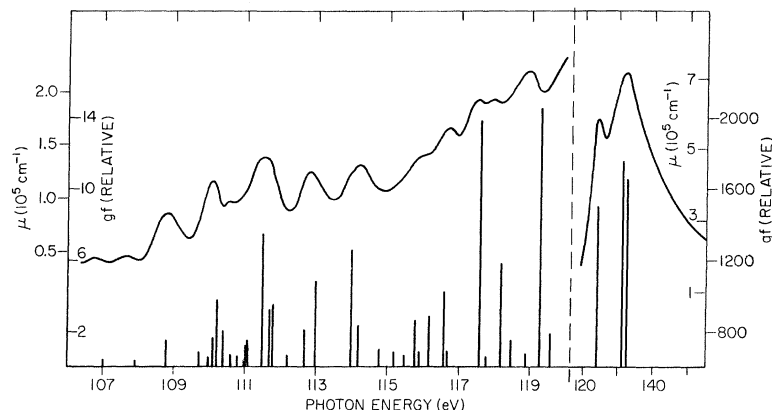


FIG. 3. Comparison of μ , the measured photon absorption coefficient for Pr in the region of the $N_{IV,V}$ edge from Ref. 2, with the calculated relative positions and gf values of the $4d^{10}4f^2 \rightarrow 4d^94f^3$ transitions.

rest of the parameters were fixed at values obtained from sources already described.

Europium is treated as a divalent case, as deduced in Ref. 5 and confirmed by the absorption data. The spectra of Eu and Gd appear to be nearly identical in Ref. 1. They belong to the isoelectronic sequence $4d^94f^8$. The fitted values of G^1 for each of these are equal, as one would expect from interactions between two inner shells where little further contraction is experienced by adding one nuclear charge. This is seen in the other fitted values of G^1 which occur from Pr onward where the collapse of the $4f$ shell is complete.

A simplification of the matrices of $4d^94f^8$ for Eu^{2+} and Gd^{3+} is used because of the unique structure of $4f^8$. There is only one term of highest multiplicity, the 7F , which is separated from the

next term by ~ 2.5 eV. Since only octet states combine with the $4d^{10}4f^7 {}^8S_{7/2}$ ground state, only lines arising from the 7F parent term appear. The large separation of the 7F from the higher terms leads to a condition of high purity for the 7F and hence to the possibility of dealing with it as an independent subconfiguration of $4f^8$. This approximation should account for the dominant structure of the absorption spectrum but certainly does not preclude the possibility of weak lines arising from higher parent terms containing a small admixture of 7F . However, the complete matrices are extremely large, and it would not have been feasible to deal with such a problem. Therefore, the analyses of Eu^{2+} and Gd^{3+} were carried out with the simplified configuration and appear to give completely adequate results.

In Table II we give the calculated energy levels,

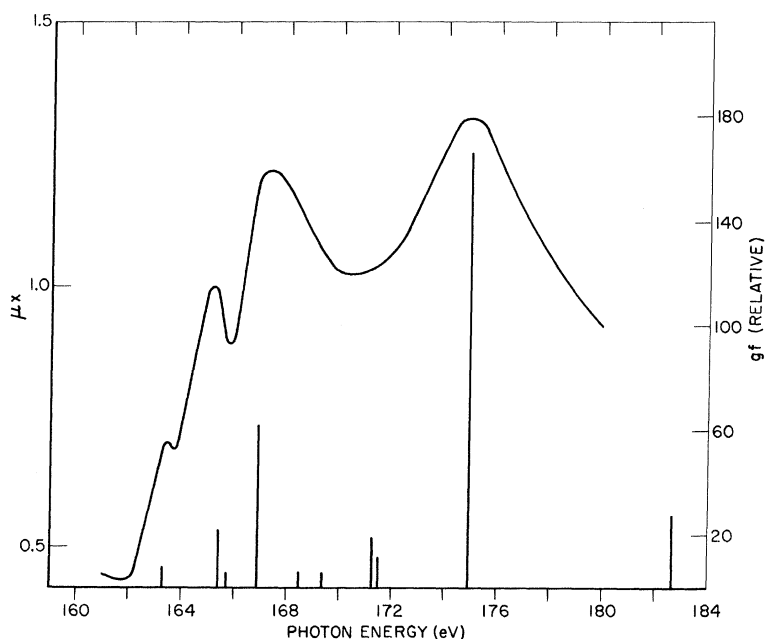


FIG. 4. Comparison of μ_x , the measured relative photon absorption coefficient for Er in the region of the $N_{IV,V}$ edge from Ref. 1, with the calculated relative positions and gf values of the $4d^{10}4f^{11}4f_{15/2} \rightarrow 4d^94f^{12}$ transitions.

TABLE I. Final radial parameter values used in diagonalization of $4d^9 4f^{N+1}$ energy matrices. Standard errors are given for values fitted by least squares to observed data. All values are in eV units.

	La $4d^9 4f$	Ce $4d^9 4f^2$	Pr $4d^9 4f^3$	Eu ^a $4d^9 4f^8$	Gd ^a $4d^9 4f^8$	Ho $4d^9 4f^{11}$	Er $4d^9 4f^{12}$	Tm $4d^9 4f^{13}$
F^2	10.2	10.3 ± 0.3	10.7 ± 0.6	12.5	12.5	13.2	13.8	14.2
F^4	6.5	6.6	6.8	8.0	8.0	8.4	8.8	9.1
G^1	9.42 ± 0.2	10.13 ± 0.08	11.3 ± 0.1	12.5 ± 0.4	12.4 ± 0.3	14.1	14.7 ± 0.4	14.6 ± 0.8
G^3	5.90	6.36	7.12	7.85	7.81	8.88	9.26	9.20
G^5	4.17	4.49	5.03	5.57	5.52	6.27	6.54	6.50
ζ_d	1.20	1.35	1.52	2.22	2.42	3.05	3.28	3.52
ζ_f	0.080	0.092	0.113	0.174	0.236	0.295	0.327	0.361
E^1		0.616	0.632			0.854	0.896	
E^2		0.003	0.003			0.004	0.004	
E^3		0.060	0.068			0.080	0.084	

^aOnly lowest $4f^8$ parent term was used. Hence, no E^i parameters were needed.

the calculated weighted oscillator strengths (gf), and the observed absorption peaks. For all cases but Er and Tm the data fall into separate regions of low and high absorption, separated in Table II by a dotted line. On either side, all calculated levels are given whose gf values are at least 5% of the largest value in that region. The scale for each element is chosen to approximate the relative peak values indicated in Ref. 1. The experimental data are taken from Ref. 2 for Ce and Pr because the resolution is improved over the data of Ref. 1.

These results differ somewhat from those given in Ref. 3. There, only the data for Ce were fitted by least squares. Then La, Er, and Tm were calculated with F^k and G^k parameters reduced from the HF values by the same percentages indicated in Ce. Some minor changes were made in the assignment of peaks to calculated levels in Ce, resulting in slight changes in the Slater integrals.

One of the weak peaks in La and Eu could not be interpreted and are included in Table II without designation. All other peaks may be attributed to the calculated structure as arising from a single level or a group of bracketed levels. The over-all accuracy of the predicted positions (rms error) varies from 0.2 to 0.3 eV. Two notable exceptions are the high-energy peaks of Ce and Ho. For Ce, the peak results from a blend of three strong lines in an interval of 5 eV. For Ho, the measurement appears to correspond to the average of a double peak shown in Ref. 1. The calculation suggests the possibility of a triple peak with an average position at the measured value.

The first column of Table II contains final-state designations that in many cases are only nominal; that is, the composition of the eigenvector shows no component reaching 50%. Even in the complex configurations of this group, however, the stronger lines usually arise from high-purity levels. This is true of the levels responsible for the strong absorption peaks.

L-S COUPLING

The coupling scheme is $L-S$ because of the dominant role of the exchange interaction. For the less than half-filled $4f$ shell the intensities are controlled by the exchange parameter G^1 in a way that preserves the $4d^9 4f$ parentage. In La^{3+} the ground state is $4d^{10} 1S_0$. The excited configuration is $4d^9 4f$, and practically all the line strength goes into the $1S_0-1P_1$ transition. This results in the strong absorption peak at 117 eV and the two weak lines at lower energy due to a slight admixture of $1P_1$ into the two triplet states. Coupling an additional f electron to the $4d^9 4f$ system mainly through the exchange interaction G^1 produces $2D$, $2F$, and G^2 terms with the $1P$ parentage. Nearly all the line strength is now distributed among these three terms, producing the three strong lines in the Ce spectrum that blend into the strong absorption peak at 124.3 eV. The relative intensity distribution within each of the $J = \frac{3}{2}$, $\frac{5}{2}$, and $\frac{7}{2}$ files can, in fact, be obtained by transforming the energy matrices to a new basis in which the base vectors are pure states of the scheme $\langle (d^9 f) S_1 L_1, f, SL \rangle$. The transformation matrix is the set of eigenvectors obtained by diagonalizing the energy matrices with all parameters zero except for G^1 , the parameter which uniquely determines the $1P$ energy. Then the percentage distribution of the $1P_1$ parent state among the eigenvalues in a physical diagonalization in the new basis closely approximates the calculated distribution of line strength in each J . For Pr, a similar procedure works equally well. The relative line strengths among the different J matrices is preserved, and so the pure $L-S$ line strengths can be summed to determine these ratios.

This coupling structure probably contributes to the decreasing intensity of the main absorption peak with increasing N . The levels arising from the $1P$ parent are distributed among more and more levels whose J values and spins do not allow elec-

TABLE II. Calculated absorption maxima (upper energy levels) and relative gf values for lanthanides near $4d$ edge. Positions of peaks (in eV) are given whose gf values are $\geq 5\%$ of maximum peak in regions of low and high absorption, separated by dotted line. Measured peak positions appear in last column.

Transition	E_{calc}	gf Rel.	E_{obs}
$\text{La}^{3+} 4d^{10} \quad {}^1S_0^-$			
$4d^9 4f \quad {}^3P_1$	97.2	1.0	96.9
3D_1	101.3	11.1	101.6
	...		103.7 ^a
1P_1	117.0	1993	117
$\text{Ce}^{3+} 4d^{10} 4f \quad {}^2F_{5/2^-}$			
$4d^9 4f^2 \quad ({}^3H) {}^4F_{3/2}$	101.8	0.2	101.25
$({}^1I) {}^2G_{7/2}$	103.5	0.9	103.48
$({}^3H) {}^4G_{5/2}$	103.7	0.5	
$({}^3H) {}^4G_{5/2}$	104.4	0.8	104.56
$({}^3H) {}^4G_{7/2}$	104.6	1.2	
$({}^1D) {}^2D_{5/2}$	105.4	1.4	105.77
$({}^3F) {}^4G_{7/2}$	105.7	6.8	
$({}^3F) {}^4G_{5/2}$	106.0	2.0	106.06
$({}^3F) {}^4F_{3/2}$	106.2	1.1	
$({}^3H) {}^4H_{7/2}$	106.6	0.5	106.58
$({}^3F) {}^4H_{7/2}$	106.8	3.4	
$({}^1G) {}^2D_{5/2}$	108.0	0.7	108.06
$({}^3P) {}^4D_{3/2}$	108.2	2.2	
$({}^3F) {}^4D_{7/2}$	108.3	0.8	108.93
$({}^3F) {}^4D_{5/2}$	108.5	0.7	
$({}^3F) {}^4D_{7/2}$	108.8	1.3	109.70
$({}^3P) {}^4P_{3/2}$	109.5	1.6	
$({}^3P) {}^4F_{7/2}$	109.8	2.0	110.36
$({}^1D) {}^2P_{3/2}$	110.0	0.6	
$({}^3F) {}^4H_{7/2}$	110.1	10.4	111.52
$({}^1D) {}^2G_{7/2}$	111.7	4.6	
	...		
$({}^3H) {}^2G_{7/2}$	120.4	1088	124.3
$({}^3F) {}^2D_{3/2}$	124.4	781	
$({}^3F) {}^2D_{5/2}$	124.8	40	125.4
$({}^3H) {}^2F_{5/2}$	125.3	1215	
$({}^3H) {}^2F_{7/2}$	125.4	85	
$\text{Pr}^{3+} 4d^{10} 4f^2 \quad {}^3H_4^-$			
$4d^9 4f^3 \quad ({}^4I) {}^5H_3$	107.0	0.5	106.70
$({}^4I) {}^5G_3$	107.9	0.5	107.70
$({}^4I) {}^3I_5$	108.8	1.5	108.83
$({}^4G) {}^5G_3$	109.7	0.9	110.12
$({}^2D1) {}^3F_4$	110.0	0.4	
$({}^4I) {}^5I_4$	110.1	1.7	110.54
$({}^4F) {}^5I_5$	110.2	3.7	
$({}^4I) {}^5I_4$	110.4	2.	110.7
$({}^2K) {}^3I_5$	110.6	0.7	
$({}^4I) {}^5G_5$	110.8	0.6	111.53
$({}^4F) {}^5G_4$	111.0	0.5	
$({}^2G1) {}^3H_5$	111.1	0.7	111.5
$({}^4F) {}^5G_3$	111.1	0.5	
$({}^4F) {}^5H_4$	111.2	1.4	111.53
$({}^2H2) {}^3G_4$	111.3	0.7	
$({}^4I) {}^5K_5$	111.5	7.5	111.53
$({}^4G) {}^3I_5$	111.6	3.2	
$({}^1I) {}^5I_4$	111.8	3.4	112.3
$({}^2H2) {}^3F_3$	112.3	0.7	

TABLE II. (Continued)

Transition	E_{calc}	gf Rel.	E_{obs}
$({}^2D2) {}^3G_5$	112.7	2.4	
$({}^4I) {}^3I_5$	113.0	4.8	112.81
$({}^4G) {}^3I_5$	114.0	6.6	114.16
$({}^4D) {}^5G_3$	114.2	2.3	
$({}^2H1) {}^3H_4$	114.8	1.1	
$({}^4G) {}^3F_3$	115.2	0.8	
$({}^2D2) {}^3F_4$	115.3	0.6	
$({}^2D2) {}^1F_3$	115.5	0.7	
$({}^4G) {}^5I_4$	115.8	2.6	115.93
$({}^4F) {}^5P_3$	115.9	0.9	
$({}^4G) {}^5I_5$	116.2	2.8	
$({}^2H1) {}^1H_5$	116.6	4.2	116.74
$({}^2G2) {}^3F_3$	116.7	0.8	
$({}^2I) {}^3I_5$	117.6	12.7	117.49
$({}^4D) {}^3G_3$	117.8	0.6	
$({}^2G2) {}^3G_5$	118.2	5.8	118.02
$({}^4D) {}^3D_3$	118.5	0.7	
$({}^2F2) {}^3H_4$	118.6	0.8	
$({}^4D) {}^3D_3$	118.9	0.7	
$({}^2F1) {}^3H_5$	119.3	12.3	118.90
	...		
$({}^4I) {}^3I_5$	124.0	1505	123.9 ^b
$({}^4G) {}^3G_3$	127.4	126	
$({}^2G2) {}^1G_4$	131.2	439	131.4
$({}^4I) {}^3H_4$	131.5	1763	
$({}^4I) {}^3H_5$	131.8	88	
$({}^4I) {}^3G_3$	133.1	1650	
$\text{Eu}^{2+} 4d^{10} 4f^7 \quad {}^8S_{7/2^-}$			
$4d^9 4f^8$			131.1 ^a
$({}^1F) {}^8D_{9/2}$	132.4	7.7	132.3
$({}^1F) {}^8D_{7/2}$	132.6	6.2	
$({}^1F) {}^8D_{5/2}$	132.8	2.6	133.6
$({}^1F) {}^8H_{9/2}$	133.3	0.7	
$({}^1F) {}^8H_{7/3}$	134.0	0.7	134.3
$({}^1F) {}^8F_{9/2}$	134.8	4.6	135.5
$({}^1F) {}^8F_{7/2}$	135.2	2.3	
$({}^1F) {}^8F_{5/2}$	135.4	0.5	136.8
$({}^1F) {}^8G_{9/2}$	136.8	5.2	
$({}^1F) {}^8G_{7/2}$	137.2	1.1	
	...		
$({}^1F) {}^6P_{7/2}$	138.7	144	142
$({}^1F) {}^6P_{5/2}$	139.5	246	
$({}^1F) {}^6P_{3/2}$	141.9	523	142.8
$({}^1F) {}^6P_{1/2}$	142.3	343	
$({}^1F) {}^6P_{5/2}$	142.6	160	142.8
$({}^1F) {}^6F_{7/2}$	145.7	40	
$({}^1F) {}^6F_{9/2}$	146.1	88	144.3
$({}^1F) {}^6D_{9/2}$	148.2	74	
$\text{Gd}^{3+} 4d^{10} 4f^7 \quad {}^8S_{7/2^-}$			
$4d^9 4f^8$			
$({}^1F) {}^8D_{9/2}$	139.6	17.9	139.5
$({}^1F) {}^8D_{7/2}$	139.8	13.8	
$({}^1F) {}^8D_{5/2}$	140.0	5.6	140.9
$({}^1F) {}^8H_{9/2}$	140.6	1.8	
$({}^1F) {}^8H_{7/2}$	141.4	0.9	141.5
$({}^1F) {}^8F_{9/2}$	142.0	11.5	142.8
$({}^1F) {}^8F_{7/2}$	142.5	5.0	
$({}^1F) {}^8F_{5/2}$	142.8	1.0	144.3
$({}^1F) {}^8G_{9/2}$	144.2	14.3	

TABLE II. (Continued)

Transition	E_{calc}	gf Rel.	E_{obs}	
$(^1F) ^8G_{7/2}$	144.6	1.0		
$(^7F) ^6P_{7/2}$	145.7	319	149	
$(^1F) ^8P_{5/2}$	146.6	534		
$(^1F) ^8P_{9/2}$	149.0	1042		
$(^1F) ^8P_{7/2}$	149.6	670		
$(^1F) ^6P_{5/2}$	150.0	308		
$(^1F) ^6F_{7/2}$	152.9	103		
$(^1F) ^6F_{9/2}$	153.3	210		
$(^1F) ^6D_{7/2}$	155.4	52		
$(^1F) ^6D_{9/2}$	155.6	172		
Ho ³⁺ $4d^{10}4f^{10}$	$^5I_8^-$			
$4d^94f^{11}$	$(^4I) ^5K_9$	156.0	37	155.8
	$(^4F) ^5H_7$	156.7	141	156.9
	$(^4I) ^5L_9$	156.9	11	158.8
	$(^4F) ^5H_7$	158.6	72	
	$(^4G) ^5I_8$	159.1	31	
	$(^4G) ^5I_7$	161.7	13	
	$(^4G) ^5H_7$	162.1	16	
	$(^2K) ^3L_8$	162.7	26	
	$(^4I) ^5I_8$	163.1	97	
	$(^4I) ^5I_8$	166.0	107	
	$(^2L) ^1L_8$	167.2	27	167
	$(^4I) ^5H_7$	169.4	102	
	$(^2L) ^3M_8$	170.8	14	
	$(^4I) ^3I_7$	174.6	27	
Er ³⁺ $4d^{10}4f^{11}$	$^4I_{15/2^-}$			
$4d^94f^{12}$	$(^3H) ^4K_{17/2}$	163.3	8.3	163.4
	$(^3H) ^4K_{15/2}$	165.4	23.0	165.1
	$(^3F) ^4H_{13/2}$	165.7	5.9	167.2
	$(^3H) ^4I_{15/2}$	166.9	63.4	
	$(^3H) ^4K_{13/2}$	168.5	6.2	
	$(^3H) ^4I_{13/2}$	169.4	5.4	
	$(^1I) ^2K_{15/2}$	171.3	19.6	
	$(^1I) ^2I_{13/2}$	171.5	12.4	
	$(^3H) ^4H_{13/2}$	174.9	167	
	$(^3H) ^2I_{13/2}$	182.7	28	
Tm ³⁺ $4d^{10}4f^{12}$	$^3H_6^-$			
$4d^94f^{13}$	3H_8	171.4	31	171.6
	3H_5	174.9	13	174.6
	3G_5	178.4	111	178.5

^aNo interpretation was found for these weak lines.

^bThere appears to be a typographical error in Table I of Ref. 2. The next to last entry under Pr should be ~ 123.9 , as seen in Fig. 1.

tric dipole transitions to the ground state. Past the middle of the $4f$ shell this model breaks down because the 1P parentage cannot be traced to a single level. This can be seen in the d^9f^{13} (or df) matrices where G^1 contributes to all terms.

Another feature of the distribution of absorption lines is noteworthy. For the less than half-filled $4f$ shell the interval between the onset of absorption and the big peak is ~ 20 eV. This abruptly

drops to ~ 10 eV past the middle of the $4f$ shell. This may be interpreted in terms of the effect of G^1 on the energy levels of d^9f^N , ignoring all other interactions. For $N < 7$ the levels contributing to the main absorption are based on the 1P of d^9f , and remain at about the same high energy (~ 20 eV) relative to the onset of absorption. On the other hand, starting with d^9f^{13} , the oscillator strength is divided between the 3H and 3G terms in the ratio of $\sim 1:3$. These terms are separated by ~ 10 eV due to their dependence on G^1 . In Er and Ho the energy separation and division of oscillator strength is about the same as in Tm, suggesting that the d^9f^{13} structure is preserved as holes are added to the $4f$ shell. This is similar to the situation described earlier for the less than half-filled shell where the d^9f structure is preserved. The parameter G^1 dominates the structure in both cases but the dependence on G^1 is different for the parentage at the two ends of the shell. The exception to this description is Gd, where the energy separation is ~ 10 eV but most of the oscillator strength is in the high-energy peak.

CONCLUSION

Recent results obtained by Brewer,¹⁶ combining thermodynamic properties of the lanthanides with spectroscopic data, support the conclusion that three electrons are effectively removed from the free atom to the valence band in forming metallic lanthanides. He shows that in order to obtain the bonding energy of the metallic lanthanides having hexagonal crystal structure one must add the energy of excitation required to form a $4f^{N-1}5d6s6p$ configuration (N equals the total number of $4f$ electrons in the ground state of the gaseous atom) to the enthalpy of sublimation. This is due to the fact that the ground electronic state of the gaseous atom differs from its normal state in the metal. "The correct measure of the cohesive energy is the enthalpy of sublimation to a gaseous atom with the same electronic configuration as in the metal."¹⁶ The valency is determined by the number of non- f -electrons.

It is clear from the simpler spectra studied in the present paper, such as La, Er, Tm, and Yb, that no other ionization stage could account for all the observed data. For La³⁺ and Tm³⁺ only three lines are allowed and only three are observed (except for the extra small peak in La³⁺). If the atoms were doubly ionized, the La spectrum would look like that shown in Fig. 2, which is far more complicated. On the other end of the period, Tm would have only one line, arising from the transition $4d^{10}4f^{13}^2F_{7/2} - 4d^94f^{14}^2D_{5/2}$. This single line is observed¹⁷ as expected in Yb. Similar arguments may be made to eliminate other stages of ionization. These results bear out in a striking way the assump-

tion on which this calculation is based, namely, that the lanthanides give up three electrons for bonding in the metal. The present interpretation of the absorption spectra provides the most detailed confirmation of this.

The lanthanides that remain to be treated and for which the data are available in Refs. 1 and 2 are Nd, Sm, and Dy. These are complex cases because of the size of the matrices needed but the methods of treatment are the same. The lanthanides show this detailed structure because the unfilled $4f$ shell is collapsed and therefore not subject to large interactions with the environment, and because of the large electrostatic interaction with the $4d$ shell.

The same set of circumstances probably exists in the actinides where the interaction is between the $5d$ and $5f$ shells. It would therefore be of interest to see the absorption experiments carried out for the actinide period.

ACKNOWLEDGMENTS

I am pleased to thank Professor Ugo Fano who brought this problem to my attention and suggested the approach which led to these results, Dr. Robert Cowan for kindly providing an independent calculation of the relative intensities in Pr utilizing the parameters given here, and Dr. John Cooper for rewarding discussions.

¹J. M. Zimkina, V. A. Fomichev, S. A. Gribovskii, and I. I. Zhukova, *Fiz. Tverd. Tela* **9**, 1447 (1967); **9**, 1490 (1967) [*Sov. Phys. Solid State* **9**, 1128, (1967); **9**, 1163 (1967)].

²R. Haensel, P. Rabe, and B. Sonntag, *Solid State Commun.* **8**, 1845 (1970).

³J. L. Dehmer, A. F. Starace, U. Fano, J. Sugar, and J. W. Cooper, *Phys. Rev. Letters* **26**, 1521 (1971).

⁴A. F. Starace, preceding paper, *Phys. Rev. B* **5**, 1773 (1972), Paper I of this series.

⁵W. H. Zachariasen, in *The Metal Plutonium*, edited by A. S. Coffinberry and W. R. Miner (University of Chicago Press, Chicago, 1961), p. 99.

⁶W. T. Carnall, P. R. Fields, and K. Rajnak, *J. Chem. Phys.* **49**, 4424 (1968); **49**, 4443 (1968); **49**, 4447 (1968); **49**, 4450 (1968).

⁷G. Racah, *Phys. Rev.* **62**, 438 (1942); **63**, 367 (1943); **76** 1352 (1949).

⁸U. Fano, F. Prats, and Z. Goldschmidt, *Phys. Rev.* **129**, 2643 (1963).

⁹A. P. Jucys, J. B. Ievinsonas, and V. V. Vanagas,

Mathematical Apparatus of the Theory of Angular Momentum, Publ. No. 3 (Akad. Nauk. Lit. SSR Inst. Fiz. Mat., Vilnius, USSR, 1960).

¹⁰C. W. Nielson and G. F. Koster, *Spectroscopic Coefficients for the p^N , d^N , and f^N Configurations* (MIT Press, Cambridge, Mass., 1963).

¹¹G. Racah, *Bull. Res. Council Israel* **8F**, 1 (1959).

¹²C. Froese, *Can. J. Phys.* **41**, 1895 (1963).

¹³J. A. Bearden, *Rev. Mod. Phys.* **39**, 78 (1967).

¹⁴J. Sugar and V. Kaufman (unpublished).

¹⁵R. D. Cowan, *J. Opt. Soc. Am.* **58**, 808 (1968).

¹⁶L. Brewer, *J. Opt. Soc. Am.* **61**, 1101 (1971).

¹⁷In Refs. 5 and 16 it is pointed out that Yb should be divalent in the metal. As such, it should show no absorption since the $4f$ shell would be full. It has been reported that absorption from the $3d$ shell in Yb occurs as one line in the oxide but not at all in the metal [F. H. Combley, E. A. Stewardson, and J. E. Wilson, *J. Phys. B* **1**, 120 (1968)]. It would therefore appear that the Yb absorption reported in Ref. 1 arose from the trivalent oxide.

Potential-Barrier Effects in Photoabsorption. III. Application to $4d$ -Shell Photoabsorption in Lanthanum[†]

J. L. Dehmer*[‡] and A. F. Starace^{§¶}

Departments of Physics and Chemistry, University of Chicago, Chicago, Illinois 60637

(Received 28 June 1971)

An exploratory calculation of the photoabsorption cross section near the $4d$ ionization threshold of lanthanum metal is carried out. The level structure of the configuration $4d^9 4f$ is found to be altered by interaction with the continuum configuration $4d^9 \epsilon f$. The Fano profile of the resonance above threshold is calculated, as are the oscillator strengths of the discrete states below threshold. Our results provide the ground work for more detailed calculations.

I. INTRODUCTION

This paper presents exploratory theoretical calculations of the $4d$ -shell photoabsorption spectrum in lanthanum, primarily to illustrate the general theory for such spectra presented in Paper

I of this series.¹ The experimental data of Zimkina *et al.*² for La exhibit a 44.5-Mb peak about 13 eV above threshold, and three weak lines within a few eV below threshold. These structures have been interpreted in a preliminary report³ as being due to $4d^{10} \rightarrow 4d^9 4f$ dipole transitions. These transitions